

More Neutrinos
+ More Space Dimensions
= More² New Physics

Tom Weiler
Vanderbilt University

Outline

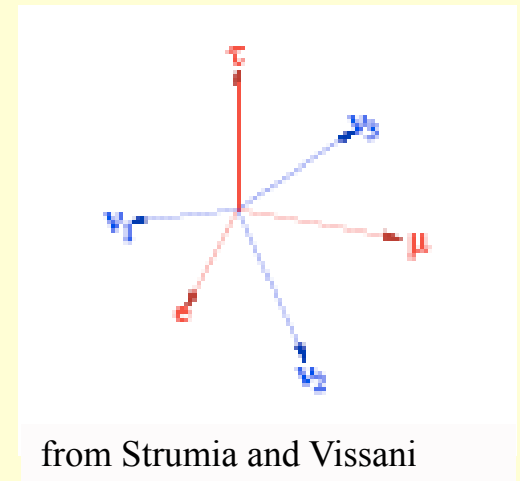
- * Neutrinos, what we know (a lot)
- * LSND/MiniBooNE and the LSND-ino/miniBooNE-ino
- * Other uses of sterile neutrinos (parameters)
- * Before MiniBooNE, there was the
PPW (Pas, Pakvasa, Weiler) prediction
- * Now comes, BMLMPPW
(Barger, Huber, Learned, Marfatia, PPW)
In with a flurry, out like a flake?
- * Closed Timelike Curves and “Time Travel”

What we know:

Three mixing angles and a phase comprise the conventional parametrization of the vacuum mixing matrix, as established by the Particle Data Group (PDG) [2]:

$$U = R_{32}(\theta_{32}) U_{\delta}^{\dagger} R_{13}(\theta_{13}) U_{\delta} R_{21}(\theta_{21}) \quad (1)$$
$$= \begin{pmatrix} c_{21}c_{13} & s_{21}c_{13} & s_{13}e^{-i\delta} \\ -s_{21}c_{32} - c_{21}s_{32}s_{13}e^{i\delta} & c_{21}c_{32} - s_{21}s_{32}s_{13}e^{i\delta} & s_{32}c_{13} \\ s_{21}s_{32} - c_{21}c_{32}s_{13}e^{i\delta} & -c_{21}s_{32} - s_{21}c_{32}s_{13}e^{i\delta} & c_{32}c_{13} \end{pmatrix}$$

where $R_{jk}(\theta_{jk})$ describes a rotation in the jk -plane through angle θ_{jk} , $U_{\delta} = \text{diag}(e^{i\delta/2}, 1, e^{-i\delta/2})$, and $s_{jk} = \sin \theta_{jk}$, $c_{jk} = \cos \theta_{jk}$. We have omitted two additional Majorana phases, as they do not affect neutrino oscillations.



We know (continued)

flavor fits to data give the following (1σ) and 3σ ranges for the PDG mixing angles [3]:

$$\begin{aligned} \sin^2 \theta_{21} &= 0.32 (\pm 0.02) \begin{matrix} +0.08 \\ -0.06 \end{matrix}, \\ \sin^2 \theta_{32} &= 0.45 (\pm 0.07) \begin{matrix} +0.20 \\ -0.13 \end{matrix}, \\ \sin^2 \theta_{13} &< (0.02) 0.050. \end{aligned} \quad (6)$$

The central values of these inferred mixing angles are quite consistent with the TriBiMaximal values [4], given

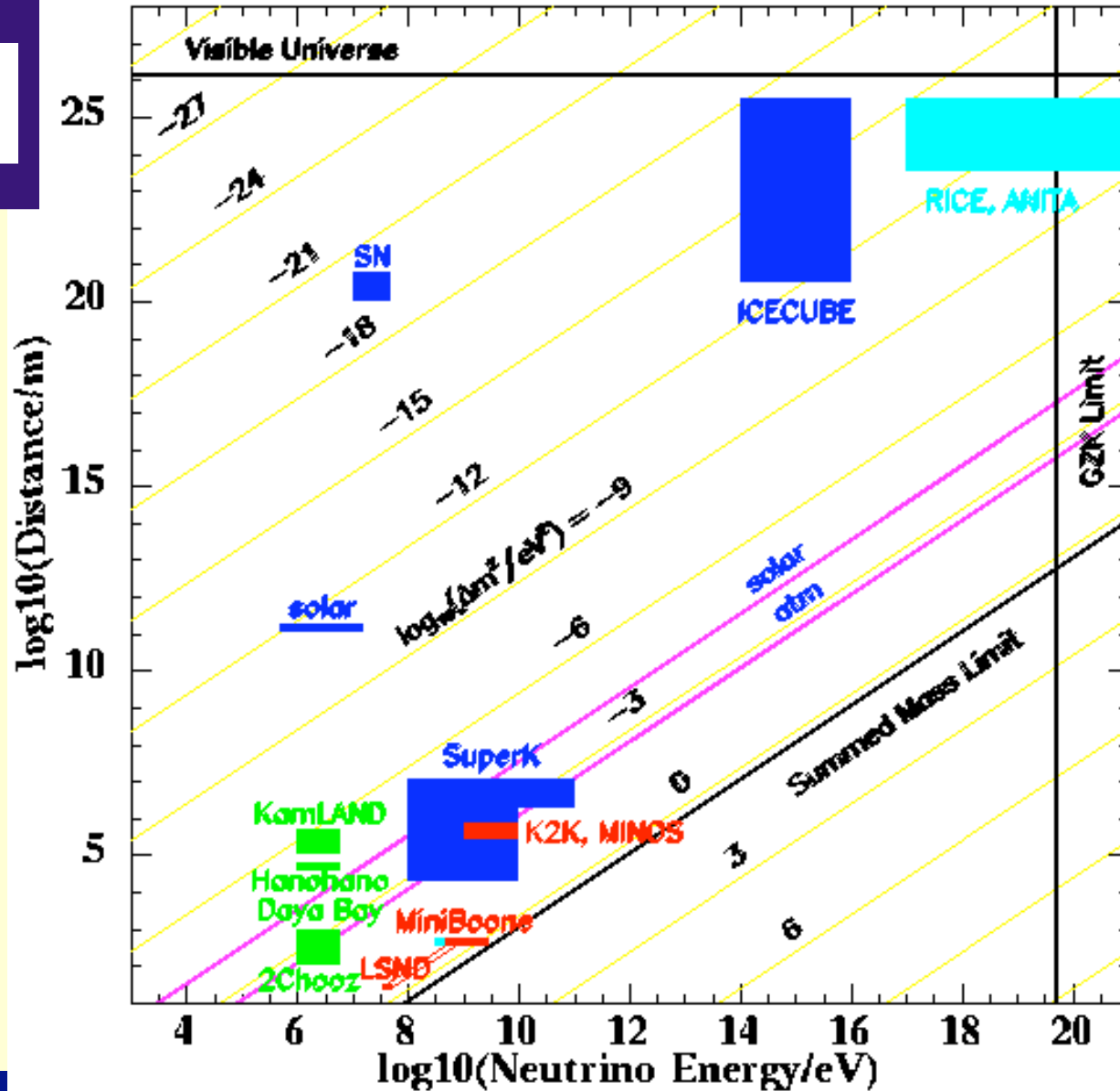
$$U_{\text{TBM}} = R_{32} \left(\frac{\pi}{4} \right) R_{21} \left(\sin^{-1} \frac{1}{\sqrt{3}} \right) = \frac{1}{\sqrt{6}} \begin{pmatrix} 2 & \sqrt{2} & 0 \\ -1 & \sqrt{2} & \sqrt{3} \\ 1 & -\sqrt{2} & \sqrt{3} \end{pmatrix}$$



Figure 2.4: Possible neutrino spectra: (a) normal (b) inverted.

Learned Plot

$$\Phi = \frac{L\delta m^2}{2E} = \left(\frac{\delta m^2}{2}\right)\left(\frac{L}{E}\right)$$



TriMinimal Parametrization of Neutrino Mixing

Pakvasa, Rodejohann,
TJW PRL (2008)

The TriMinimal parametrization is given by

$$\begin{aligned} U_{\text{TMIn}} &= R_{32} \left(\frac{\pi}{4} \right) U_e(\epsilon_{32}; \epsilon_{13}, \delta; \epsilon_{21}) R_{21} \left(\sin^{-1} \frac{1}{\sqrt{3}} \right) \\ &= \begin{pmatrix} \sqrt{2} & 0 & 0 \\ 0 & 1 & 1 \\ 0 & -1 & 1 \end{pmatrix} \frac{U_e}{\sqrt{6}} \begin{pmatrix} \sqrt{2} & 1 & 0 \\ -1 & \sqrt{2} & 0 \\ 0 & 0 & \sqrt{3} \end{pmatrix}, \end{aligned}$$

$$\text{with } U_e = R_{32}(\epsilon_{32}) U_\delta^\dagger R_{13}(\epsilon_{13}) U_\delta R_{21}(\epsilon_{21}) \quad (8)$$

chosen to have just the form of the PDG parametrization. And just as in the PDG parametrization, U_e is unitary, and therefore so is TriMinimal U_{TMIn} . The simplicity of Eq. (8) is a fortuitous result of the fact that it is the middle rotation angle (θ_{13}) in the PDG parametrization that is set identically to zero in the TriBiMaximal scheme.

the small ϵ_{jk} are obtained from the (1σ) 3σ ranges of the large oscillation angles in Eq. (6). The allowed ranges are:

$$-0.08 \text{ } (-0.04) \leq \epsilon_{21} \leq (0.01) \text{ } 0.07, \quad (13)$$

$$-0.18 \text{ } (-0.10) \leq \epsilon_{32} \leq (0.04) \text{ } 0.15, \quad (14)$$

$$|\epsilon_{13}| \leq (0.14) \text{ } 0.23, \quad (15)$$

while the CP-invariant lies in the range $|J_{\text{CP}}| \leq (0.03) \text{ } 0.05$.

Long-Distance QM evolves to Classical Probabilities

of classical probabilities, defined by $(\underline{U})_{\alpha j} \equiv |U_{\alpha j}|^2$. The full matrix of squared elements, through order $\mathcal{O}(\epsilon^2)$, is

$$\underline{U}_{\text{TMin}} = \frac{1}{6} \left\{ \begin{pmatrix} 4 & 2 & 0 \\ 1 & 2 & 3 \\ 1 & 2 & 3 \end{pmatrix} - E_1 \begin{pmatrix} 0 & 0 & 0 \\ -1 & 1 & 0 \\ 1 & -1 & 0 \end{pmatrix} - E_2 \begin{pmatrix} 2 & -2 & 0 \\ -1 & 1 & 0 \\ -1 & 1 & 0 \end{pmatrix} - 2\epsilon_{32} \begin{pmatrix} 0 & 0 & 0 \\ 1 & 2 & -3 \\ -1 & -2 & 3 \end{pmatrix} - \epsilon_{13}^2 \begin{pmatrix} 4 & 2 & -6 \\ -2 & -1 & 3 \\ -2 & -1 & 3 \end{pmatrix} \right\} \quad (17)$$

where $E_1 = 2\sqrt{2}\epsilon_{13}\cos\delta + 2\epsilon_{21}(\epsilon_{13}\cos\delta - 2\sqrt{2}\epsilon_{32})$, and $E_2 = 2\sqrt{2}\epsilon_{21} + \epsilon_{21}^2$. That there are four independent terms in (17) reflects the fact that there are four independent moduli in the neutrino mixing matrix [9].

Some useful results follow immediately from this matrix. For example, in models where neutrinos are unstable, only the lightest neutrino mass-eigenstate arrives at Earth from cosmically-distant sources [10]. Flavor ratios at Earth for the normal mass-hierarchy are $\underline{U}_{e1} : \underline{U}_{\mu 1} : \underline{U}_{\tau 1}$, and for the inverted mass-hierarchy are $\underline{U}_{e3} : \underline{U}_{\mu 3} : \underline{U}_{\tau 3}$. These ratios may be read off directly from the 1st and 3rd columns of Eq. (17). As another example, emanating solar neutrinos are nearly pure ν_2 mass states [11]; consequently, their flavor ratios at Earth are mainly given by the 2nd column of (17).



Figure 2.4: Possible neutrino spectra: (a) normal (b) inverted.

No- ν Double Beta-decay, Dirac versus Majorana-

If ν is Dirac, then there exist at least 2 (or 3) light sterile (gauge singlet) states!

LSND/MiniBooNE may have glimpsed the 4th.

Majorana-ness can be validated:

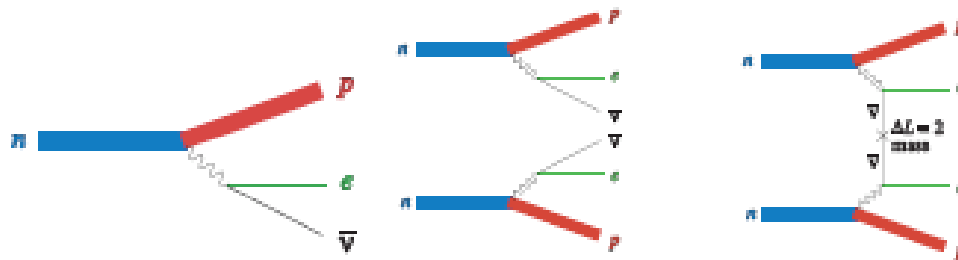
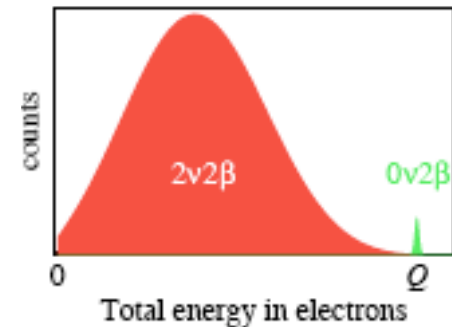


Figure 8.1: Feynman diagrams for β decay, double- β decay, and neutrino-less double- β decay.



Matter Effects and Resonance

Flavor-dependent Potential Energies $\sim G_F n_e$

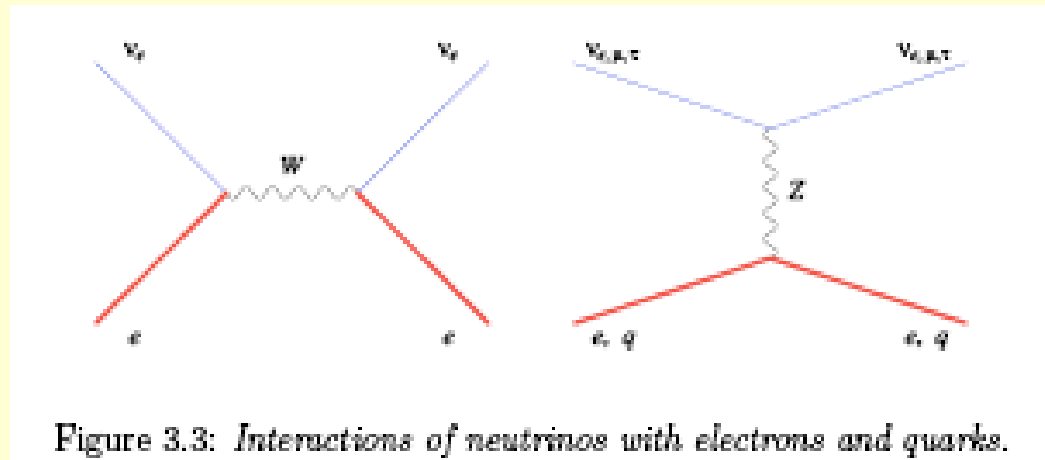


Figure 3.3: Interactions of neutrinos with electrons and quarks.

beating against Mass-dependent Kinetic Energies

$$E = \sqrt{p^2 + m^2} \sim p + m^2/2E$$

Matter-Resonances

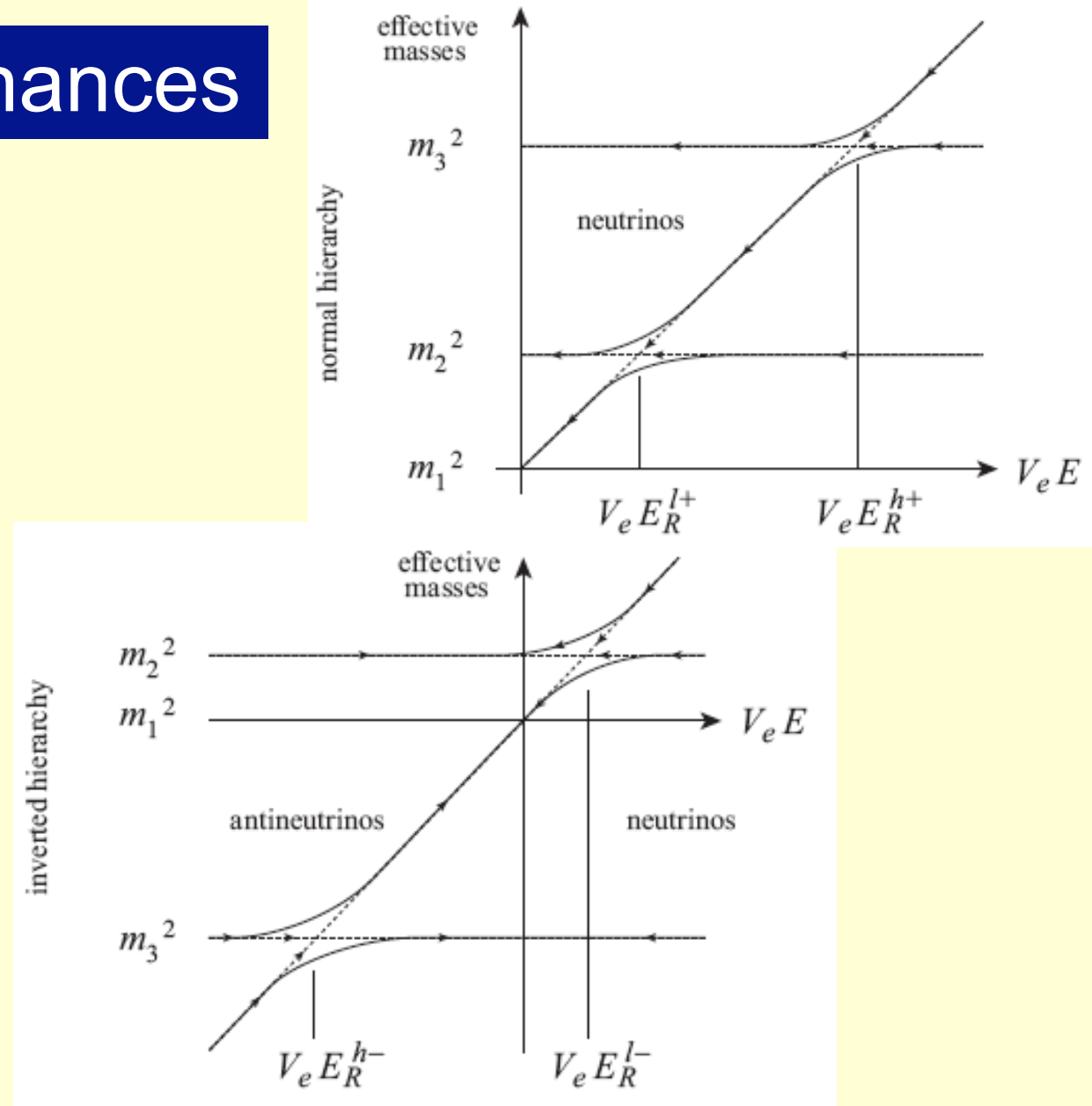


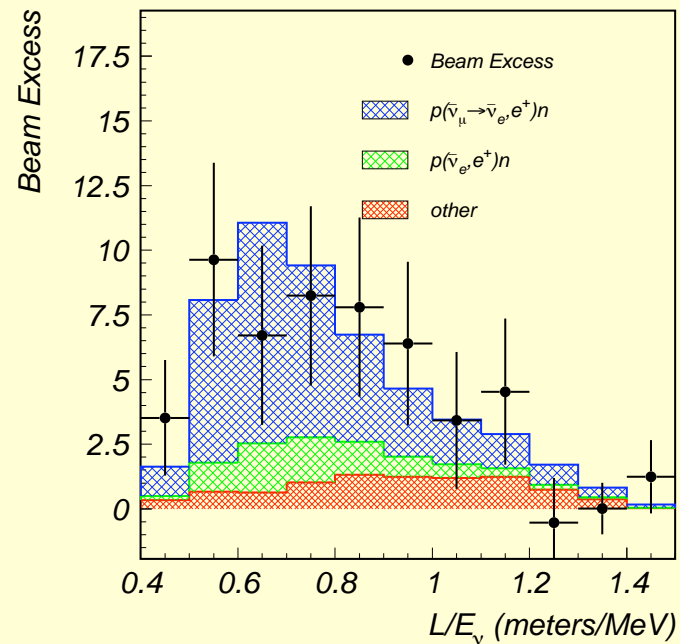
FIG. 1: Schematic illustration of the relative positions of the lower- and higher-energy resonances for the normal and inverted mass hierarchies. Neutrino (antineutrino) eigenvalues are on the right (left) of the vertical effective-mass axis. The dotted lines indicate non-adiabatic transitions.

LSND data

In the LSND [13] and KARMEN [14] experiments, a proton beam is used to produce π^+ , that decay as

$$\pi^+ \rightarrow \mu^+ \nu_\mu, \quad \mu^+ \rightarrow e^+ \nu_e \bar{\nu}_\mu$$

LSND



75 MeV

20 MeV

3+ sigma

LSND Anomaly

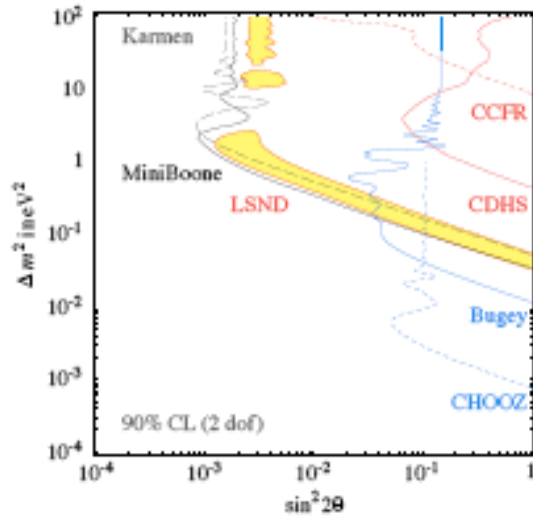


Figure 9.2: Data in the ν_e, ν_μ sector. The mixing angle θ on the horizontal axis is different for the different experiments. Bound from MINIBoONE, KARMEN and LSND region (shaded) for $\nu_\mu \rightarrow \nu_e$. Bounds from BUGEY and CHOOZ (ν_e disappearance), CDHS (ν_μ disappearance), CCFR (ν_μ disappearance). All at 90% CL (2 dof).

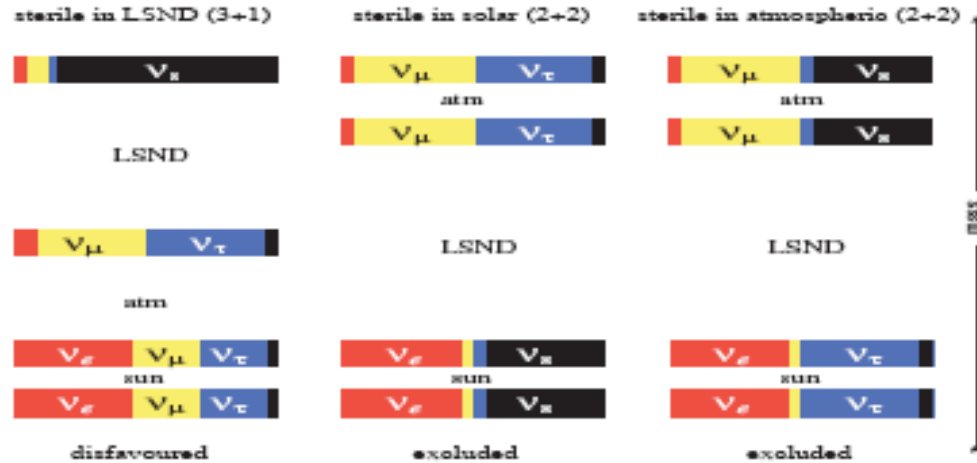


Figure 9.5: Three different mass spectra that try to explain the solar, atmospheric and LSND anomalies adding one extra sterile neutrino.

One possible global explanation of the three anomalies is that an extra sterile neutrino generates one of them. However, each anomaly, when fitted independently from the other ones, prefers active oscillations refusing the sterile neutrino. The relatively better global fit is obtained with a '3+1 spectrum' (sterile LSND oscillations) rather than with a '2+2 spectrum' (sterile solar or atmospheric oscillations).

'3+1' indicates that the additional sterile neutrino is separated by the large LSND mass gap from the 3 active neutrinos, separated among them only by the small solar and atmospheric mass differences (see fig. 9.5a). 3+1 oscillations present a phenomenological problem, because predict that $\nu_\mu \rightarrow \nu_e$ oscillations at the LSND frequency proceed through $\nu_\mu \rightarrow \nu_\tau \rightarrow \nu_e$, and $\nu_{e\mu} \rightarrow \nu_e$ oscillations are strongly constrained by disappearance experiments. Keeping only oscillations at the dominant LSND frequency

$$S \equiv \sin^2(\Delta m_{\text{LSND}}^2 L / 4E_\nu)$$

one has

$$P(\nu_e \rightarrow \nu_e) = 1 - S \sin^2 2\theta_{e\tau} \quad P(\nu_\mu \rightarrow \nu_\mu) = 1 - S \sin^2 2\theta_{\mu\tau} \quad P(\nu_e \rightarrow \nu_\mu) = S \sin^2 2\theta_{\text{LSND}}$$

with $\theta_{\text{LSND}} \approx \theta_{e\tau} \theta_{\mu\tau}$, or more precisely [92]

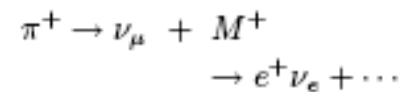
$$\sin^2 2\theta_{\text{LSND}} \simeq 4\theta_{\text{LSND}}^2 \simeq \frac{1}{4} \sin^2 2\theta_{e\tau} \sin^2 2\theta_{\mu\tau}. \quad (9.1)$$

The present constraints on the $\theta_{e\tau}$ and the $\theta_{\mu\tau}$ mixing angles are so strong that this 'product rule' prevents a clean explanation of the LSND anomaly. The $\theta_{e\tau}$ mixing angle is constrained

A Palatable Fourth Neutrino?

LSNDino Requires Way Beyond Standard Model Models:

1. ν_s and CPTV
2. $N =$ Two or more
3. Exotic pion or mu decay, e.g.



4. Xdim/Lorentz Violation/Phi-ether
(latter breaks CP, \Rightarrow nu-nubar different)

“It’s parameter-counting, stupid!”
- James Carville

Some Virtues of Sterile Neutrinos

1. With $\sim 10^{14}$ GeV mass and Yukawa's ~ 1 , see-saw mechanism for light nu mass generation
2. With \sim GeV mass and tiny Yukawa's, see-saw too (Shapashnikov's ν MSSM)
3. Supernovas and r-process nucleosynthesis (Fuller)
4. Pulsar kicks, stellar formation via H^+ , warm dark matter (Kusenko and collabs.)

Can be sought by Accelerators, but especially, if Dark Matter, via GLAST (5/16/08 launch):

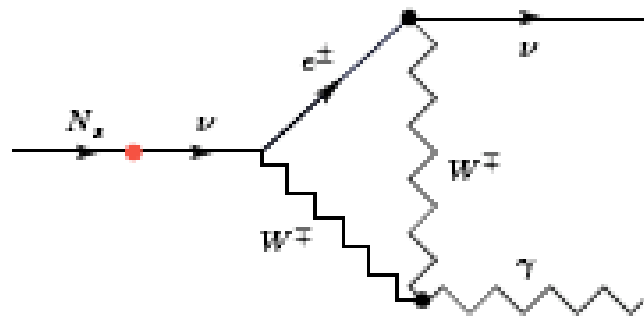


Figure 3: The one-loop diagram giving rise to radiative neutrino decay.

PPW (arXiv: hep-ph/0504096 and PRD 2005)

Sterile-active neutrino oscillations and shortcuts in
the extra dimension

Heinrich Päs¹, Sandip Pakvasa¹, Thomas J. Weiler²

Your D-brane looks like this:

In QG/String Theory, brane is dynamical, fluctuating,

due to

Quantum Mechanics

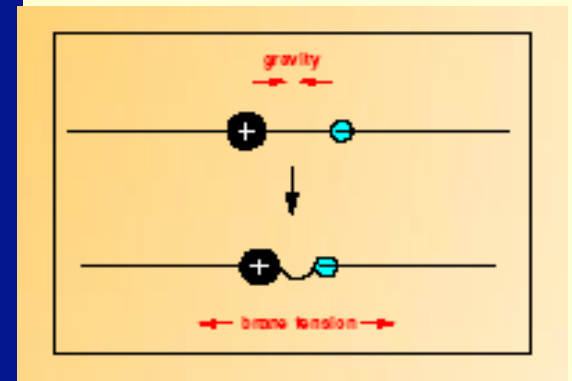
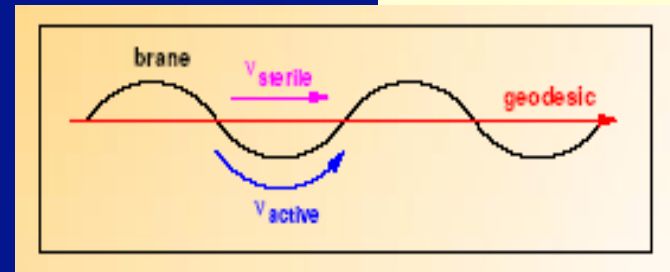
Thermal Mechanics

In-Brane stresses

(e.g. EM vs. gravity)

Out of Brane experiences

(e.g. trans-brane gravity,
or recoil against particle exodus)



Brane-Bulk resonance in two-state approximation

Define the ν_a - ν_4 projection $|\nu_a\rangle_U = |\nu_4\rangle - \langle \nu_s | \nu_4 \rangle |\nu_s\rangle$, and work with single active plus single sterile two-state system:

Evolution equation in flavor space:

$$i \frac{d}{dt} \begin{pmatrix} \nu_a(t) \\ \nu_s(t) \end{pmatrix} = H_F \begin{pmatrix} \nu_a(t) \\ \nu_s(t) \end{pmatrix}$$

Hamiltonian in the presence of bulk shortcuts:

$$\epsilon = \delta t/t = \delta x/x = \delta v/v$$

$$H_F = + \frac{\delta m^2}{4E} \begin{pmatrix} \cos 2\theta & -\sin 2\theta \\ -\sin 2\theta & -\cos 2\theta \end{pmatrix} + E \frac{\epsilon}{2} \begin{pmatrix} -1 & 0 \\ 0 & 1 \end{pmatrix}$$

\Rightarrow A Resonance exists at $E_{\text{res}} = \sqrt{\frac{\delta m^2 \cos 2\theta}{2\epsilon}}$ Energy and nu/nubar independent

\rightarrow choose $E_{\text{res}} = 60 - 500 \text{ MeV} \leftrightarrow \epsilon \simeq 10^{-18} - 10^{-16}$

epsilon

We have traded eps for E_R ,
but,

$\text{eps} = (kA/2)^2$ is itself very interesting.

[A is fluctuation amplitude, k is fluc'n wavenumber]

In the brane-fluctuation interpretation,
eps describes the geometry of the fluctuation.

One interpretation is

$kA =$ momentum recoil/brane tension,

implies tension to be of order

i.e. ~ 100 PeV

(safely above TeV EW scale)

$$\frac{E}{\sqrt{\epsilon}}$$

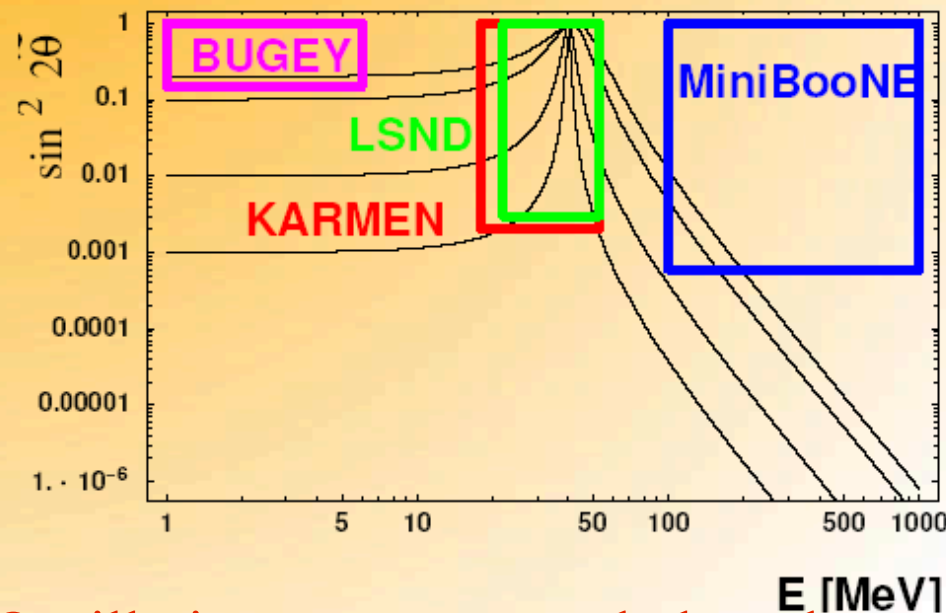
“Typical” Oscillation with Resonance

$$P_{as} = \sin^2 2\tilde{\theta} \sin^2(\delta H D/2)$$

$$\sin^2 2\tilde{\theta} = \left[\frac{\sin^2 2\theta}{\sin^2 2\theta + (\cos 2\theta - A)^2} \right]$$

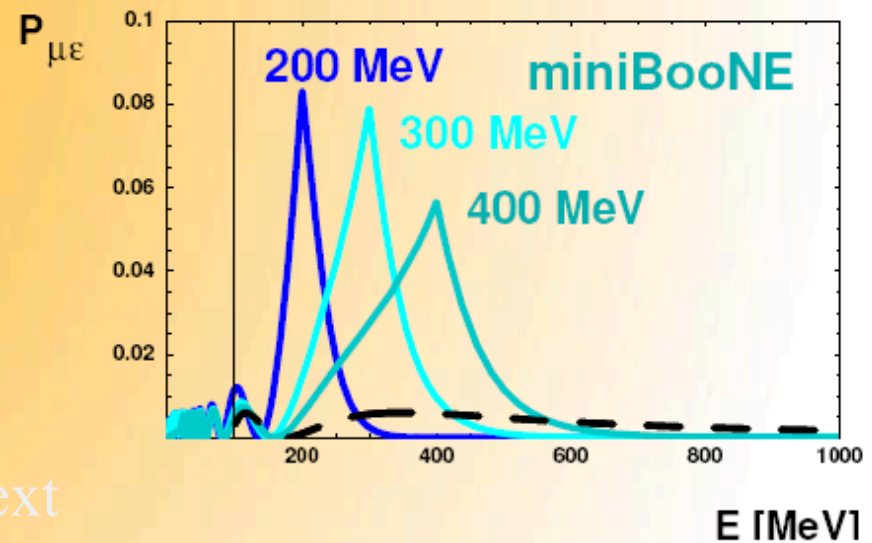
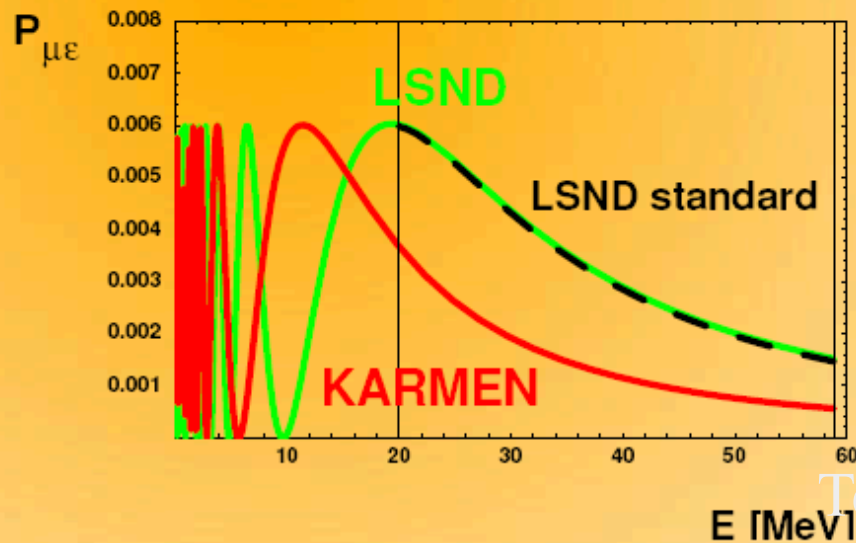
$$\delta H = \frac{\delta m^2}{2E} \sqrt{(\cos 2\theta - A)^2 + \sin^2 2\theta}$$

$$A = (E_{\text{res}}/E)^2$$



Oscillations are vacuum below the resonance, and
Oscillations at $E \gg E_{\text{res}}$ are suppressed!

Examples: few 100 MeV resonance

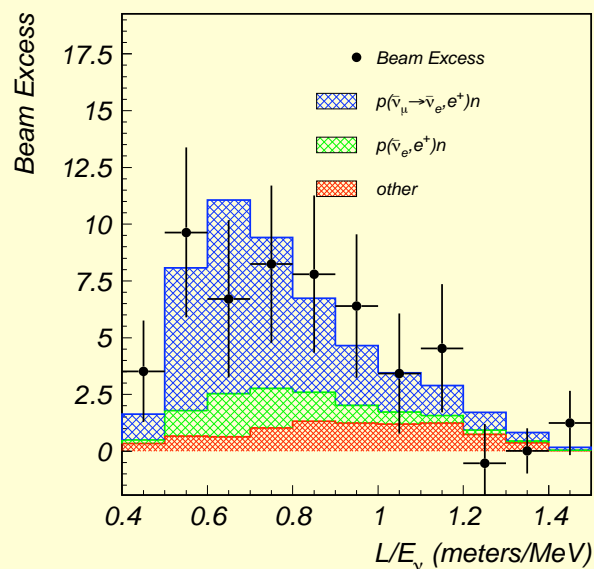


- $E_{\text{res}} = 200 \text{ MeV}, 300 \text{ MeV}, 400 \text{ MeV}; \sin^2 \theta_* = 0.1; \sin^2 2\theta = 0.45;$
 $\delta m^2 = 0.8 \text{ eV}^2$
- good fit to LSND spectrum, $P_{\text{LSND}} > P_{\text{KARMEN}}$
- enhanced miniBooNE signal in the energy range 100-600 MeV

And significant ν_μ disappearance for stopped-pion source (SNS)

LSND and MiniBooNE data

LSND

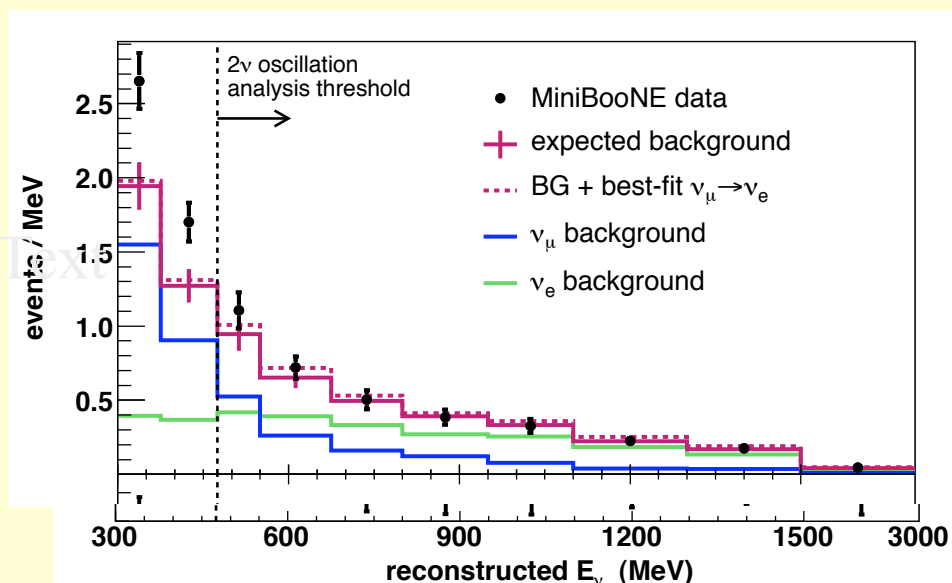


75 MeV

20 MeV

3+ sigma

MiniBooNE



3.7 sigma

Forthcoming MiniBooNE data

1. Neutrino data down to 100 MeV
2. 18 months of anti-neutrino data
3. NUMI data, at 50% that of recently published data
4. SciBooNE (detector at 100m) data
5. longer term, perhaps
 - a. the BooNE detector at a km
 - b. liquid argon R&D vessel

Oscillation Phase from Bulk Travel / LIV

$$A(\nu_\alpha \rightarrow \nu_\beta) = \langle \nu_\alpha | e^{-iHt} | \nu_\beta \rangle. \quad (1)$$

The component of Ht which is common (i.e., proportional to the identity) cannot effect flavor change, so we may subtract it. We write the remainder as $\delta(Ht)$. With the assumption that the non-common contributions are small, we may further expand $\delta(Ht)$ as $(\delta H)t + H(\delta t)$. We are left with

$$A(\nu_\alpha \rightarrow \nu_\beta) = \langle \nu_\alpha | e^{-i[(\delta H)t + H(\delta t)]} | \nu_\beta \rangle.$$

two phase sources;
can cancel each other at Resonance

As in standard oscillations, δH is diagonal in the mass-basis, and at lowest order is equal to

$$\delta H = \frac{1}{2E} \text{diag}(m_1^2, m_2^2, \dots). \quad (3)$$

Alternatively, one may view (δt) from the brane point of view as an apparent violation of Lorentz Invariance: (LIV) has been shown to be phenomenologically equivalent to state-dependent limiting velocities [3, 4]. We note that with differing velocities, one has $\delta t = \delta(L/v) = -L \delta v/v^2$, which is $-L \delta v$ to lowest order. It is most natural to assign the limiting velocities to the interaction flavor eigenstates. In this case, the second term in (2) as written is already in a diagonal basis, and is equal to

$$\delta t = \text{diag}(\delta t_\alpha, \delta t_\beta, \dots) = -L \text{diag}(\delta v_\alpha, \delta v_\beta, \dots). \quad (5)$$

Putting the two terms together, we are led to the following effective neutrino Hamiltonian in the flavor basis:

$$H_{[F]} = \frac{1}{2E} U \begin{pmatrix} m_1^2 & 0 & 0 & 0 \\ 0 & m_2^2 & 0 & 0 \\ 0 & 0 & m_3^2 & 0 \\ 0 & 0 & 0 & m_4^2 \end{pmatrix} U^\dagger - E \begin{pmatrix} \delta v_1 & 0 & 0 & 0 \\ 0 & \delta v_2 & 0 & 0 \\ 0 & 0 & \delta v_3 & 0 \\ 0 & 0 & 0 & \delta v_4 \end{pmatrix}$$

Brane-Bulk resonance with single-(new)angle assumption

With these assumptions, the effective Hamiltonian in (7) may be written as

$$H_{(F)} = \begin{pmatrix} U_{3 \times 3} & 0 \\ 0 & 1 \end{pmatrix} \left[\frac{1}{2E} \begin{pmatrix} 1 & 0 & 0 \\ 0 & 1 & 0 \\ 0 & 0 & R_{43} \end{pmatrix} \begin{pmatrix} 0 & 0 & 0 & 0 \\ 0 & 0 & 0 & 0 \\ 0 & 0 & 0 & 0 \\ 0 & 0 & 0 & \Delta_{\text{LSND}} \end{pmatrix} \begin{pmatrix} 1 & 0 & 0 \\ 0 & 1 & 0 \\ 0 & 0 & R_{43}^T \end{pmatrix} - E \epsilon \begin{pmatrix} 0 & 0 & 0 & 0 \\ 0 & 0 & 0 & 0 \\ 0 & 0 & 0 & 0 \\ 0 & 0 & 0 & 1 \end{pmatrix} \right] \begin{pmatrix} U_{3 \times 3}^\dagger & 0 \\ 0 & 1 \end{pmatrix} \quad (10)$$

where $\epsilon = (\Delta t)/t = (\Delta x)/x = (\Delta v)/v$.

The matrix in brackets in (10) is equal to [same for ν_μ and $\bar{\nu}_\mu$]

$$\frac{\Delta_{\text{LSND}}}{2E} \begin{pmatrix} 0 & 0 & 0 & 0 \\ 0 & 0 & 0 & 0 \\ 0 & 0 & s_{43}^2 & s_{43} c_{43} \\ 0 & 0 & s_{43} c_{43} & \left(c_{43}^2 - \frac{2E^2 \epsilon}{\Delta_{\text{LSND}}} \right) \end{pmatrix}, \quad (11)$$

Resonant mixing occurs when the two diagonal elements in Eq. (11) are equal, i.e. when

$$E_R = \sqrt{\frac{\cos 2\theta_{43} \Delta_{\text{LSND}}}{2\epsilon}}. \quad \text{[same for } \nu_\mu \text{ and } \bar{\nu}_\mu \text{]}$$

Parameter-count

New parameters are

1. θ_{43}

2. E_R

which together specify the running $\tan 2\tilde{\theta} = \frac{\tan 2\theta_{43}}{1 - \left(\frac{E}{E_R}\right)^2}$,

3. Δ_{LSND} , which affects resonance length

To fit

1. LSND excess spectrum

2. MiniBooNE excess, width and null spectrum

3. Bugey, CDHS, null results

4. Long-baseline Solar and Atmospheric

is Non Trivial !

Two fitting “philosophies” :

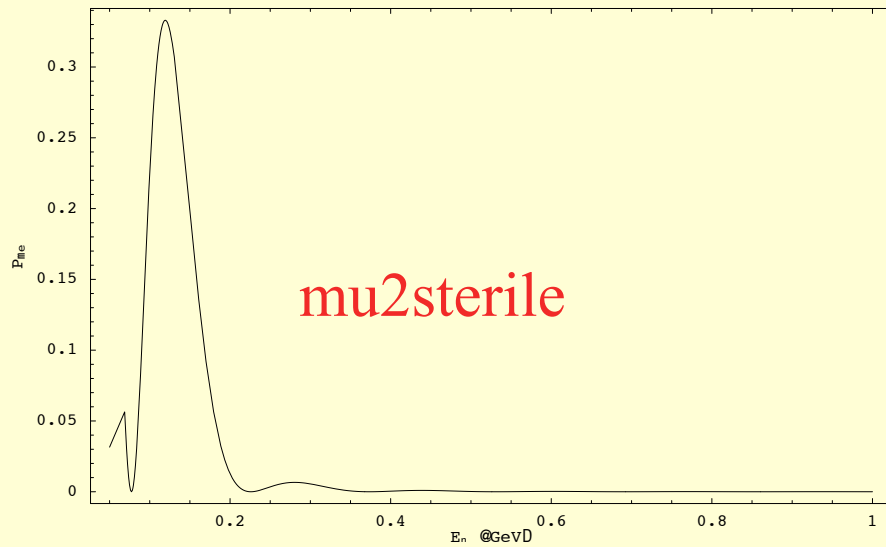
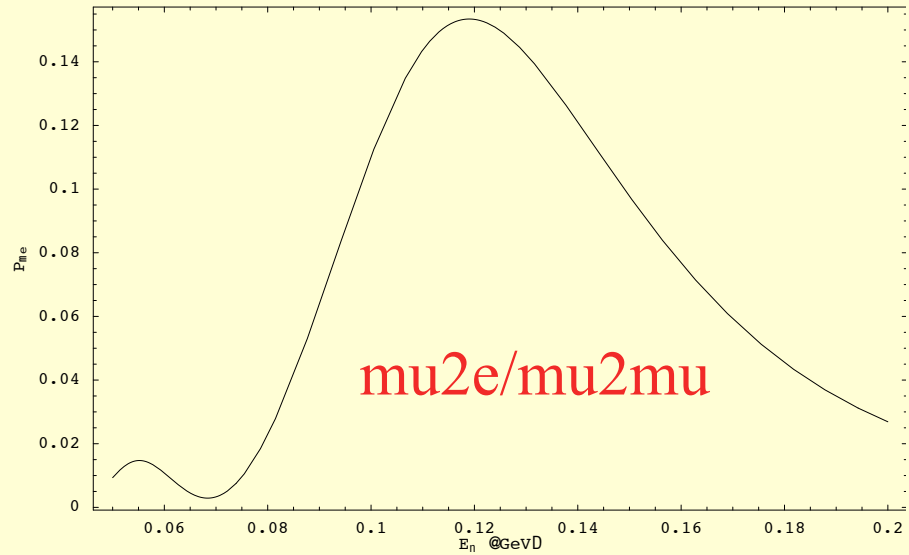
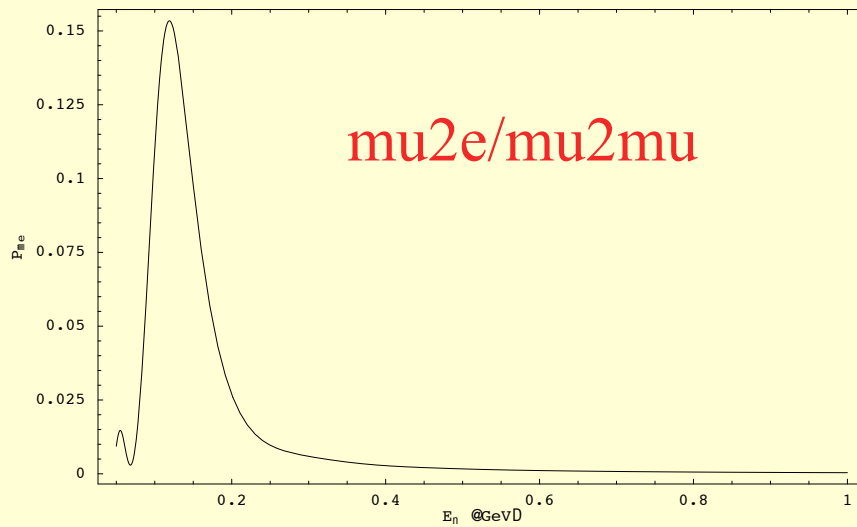
First is to fit all DATA with the three parameters, and see what happens. [Huber]

A: great chi-square and pgof, LSND is “real”, MiniBooNE is not

Second is to force a fit to LSND AND MiniBooNE excesses, and check the chisquare. [Paes and Weiler]

A: Has not yet been done, but have Paes “typical” Figures:

MiniBooNE



$$\begin{aligned}\theta_{42} &= 0.3 \text{ rad,} \\ \Delta_{\text{LSND}} &= 0.5 \text{ eV}^2, \\ E_R &= 120 \text{ MeV}\end{aligned}$$

PPW formulas

Eq. (9). The eigenvalues are

$$\lambda_1 = \lambda_2 = 0, \quad \lambda_{4/3} \equiv \lambda_{\pm} = \frac{\Delta_{\text{LSND}}}{4E} \left(1 - \cos 2\theta_{43} \left(\frac{E}{E_R} \right)^2 \pm \sqrt{\sin^2 2\theta_{43} + \cos^2 2\theta_{43} \left[1 - \left(\frac{E}{E_R} \right)^2 \right]^2} \right).$$

The eigenvalue differences $\delta H_{kj} \equiv \lambda_k - \lambda_j$ are

$$\begin{aligned} \delta H_{43} &= \lambda_+ - \lambda_- = \frac{\Delta_{\text{LSND}}}{2E} \sqrt{\sin^2 2\theta_{43} + \cos^2 2\theta_{43} \left[1 - \left(\frac{E}{E_R} \right)^2 \right]^2} \\ \delta H_{42} &= \delta H_{41} = \lambda_+ \\ \delta H_{32} &= \delta H_{31} = \lambda_- \\ \delta H_{21} &= 0 \end{aligned}$$

Just as E_R sets the energy scale for the resonance, the length scale for the resonance maximum is set by an interplay of the various

$$L_R \equiv \frac{\pi}{|\delta H_{jk}|}. \quad (24)$$

The mixing-angle dependent factors are maximized at $E = E_R$, and the length-dependent \sin^2 factor is maximized at $L \approx L_R$. Substituting $E = E_R$ into (20), and this into (24), gives the optimized length for resonance enhancement. The result is

$$L_R^{+-}(E = E_R) \equiv \frac{\pi}{\lambda_+ - \lambda_-} = \frac{2\pi}{\sin 2\theta_{43}} \frac{E_R}{\Delta_{\text{LSND}}} = \frac{500 \text{ meters}}{\sin 2\theta_{43}} \times \frac{(E_R/400\text{MeV})}{(\Delta_{\text{LSND}}/\text{eV}^2)}, \quad (25)$$

and

$$L_R^{\pm}(E = E_R) \equiv \frac{\pi}{|\lambda_{\pm}|} = \frac{4\pi}{(\sin 2\theta_{43} \pm \sin^2 \theta_{43})} \frac{E_R}{\Delta_{\text{LSND}}} \approx 2L_R^{+-}. \quad (26)$$

Since the mini-BooNE decay length is approximately 500 meters, we learn that the miniBooNE event excess around 300-400 MeV is optimized if $(\sin 2\theta_{43} \Delta_{\text{LSND}})$ is of order 1-2 eV².

PPW formulas (continued)

neutrino survival probability is given by

$$P(\nu_\alpha \rightarrow \nu_\alpha) = \delta_{\alpha\beta} - 4V_{a3}^2 \times \begin{cases} \sin^2 \left(\frac{L(\lambda_+ - \lambda_-)}{2} \right) & \sin^2 \tilde{\theta} \cos^2 \tilde{\theta} V_{a3}^2 \\ + \sin^2 \left(\frac{L\lambda_+}{2} \right) & \sin^2 \tilde{\theta} (1 - V_{a3}^2) \\ + \sin^2 \left(\frac{L\lambda_-}{2} \right) & \cos^2 \tilde{\theta} (1 - V_{a3}^2). \end{cases} \quad (26)$$

The active-to-(different)active neutrino conversion probability is given by (and note the minus sign on the first term in brackets)

$$P(\nu_\alpha \rightarrow \nu_\beta) = 4V_{a3}^2 V_{b3}^2 \times \begin{cases} - \sin^2 \left(\frac{L(\lambda_+ - \lambda_-)}{2} \right) & \sin^2 \tilde{\theta} \cos^2 \tilde{\theta} \\ + \sin^2 \left(\frac{L\lambda_+}{2} \right) & \sin^2 \tilde{\theta} \\ + \sin^2 \left(\frac{L\lambda_-}{2} \right) & \cos^2 \tilde{\theta}. \end{cases} \quad (27)$$

The active-to-sterile conversion probability is given by

$$P(\nu_\alpha \leftrightarrow \nu_s) = \sin^2(2\tilde{\theta}) V_{a3}^2 \sin^2 \left(\frac{L(\lambda_+ - \lambda_-)}{2} \right).$$

Barger, Huber, Learned, Marfatia, PPW (in progress)

Summary so far:

Bulk Travel/Lorentz Violation on the brane can yield a resonance in the 30-500 MeV region, thereby isolating low-energy LSND from “high” energy CDHS.

This may allow the 3+1 neutrino spectrum to describe all neutrino data with just one θ_{4j} [or not].

The resonance may or may not reveal itself in the intermediate energy data of MiniBoone.

The resonance certainly reveals itself in the proposed low-energy SNS-Oscillation Xpt.

The more natural model with two or three θ_{4j} angles is under investigation. It requires numerical diagonalization of a 4x4 or 3x3 mixing matrix, so few analytical insights.

Time-Travel is a chicken-wire topic



the **new**
Blues
Brothers

FAR WEST ENTERTAINMENT
P.O. BOX 55583
SEATTLE, WA 98155-0583
(206) 718-3456 FAX (206) 388-8498



Time-Traveling (research for the tenured only):

Even if chronology is protected by some mechanism operative near the chronology horizon, it remains a highly rewarding effort to study the physics near this horizon. The CTC we have constructed is particularly interesting in this respect, since it is available to particles which have previously been hypothesized to propagate in the extra-dimensional bulk². Such particles include the graviton and sterile (gauge singlet) fermions.

Classic Tipler-vanStockum and Goedel

Before discussing the causality properties of asymmetrically warped spacetimes, it is instructive to review two prominent early examples of spacetimes implementing closed time-like curves. The Gödel metric describes a pressure-free perfect fluid with negative cosmological constant and rotating matter, and the Tipler-van-Stockum spacetime is being generated by a rapidly rotating infinite cylinder. In both cases the metric can be written as

$$ds^2 = +g_{00}dt^2 + 2g_{0\phi}dtd\phi + g_{\phi\phi}d\phi^2 + \text{additional terms.} \quad (1)$$

Here the $g_{\mu\nu}$ are complicated functions of the distance to the symmetry axis, angular velocity and radius of the setup. The angular coordinate ϕ assumes values on the interval $\phi \in [0, 2\pi]$.

CTCs (continued)

The metric has Lorentzian signature provided that

$$(g_{00}g_{\phi\phi} - g_{0\phi}^2) < 0. \quad (2)$$

When we consider an azimuthal null-curve $\phi = 0 \rightarrow \phi = 2\pi$ with all other coordinates fixed, $ds^2 = 0$ implies

$$\dot{\phi} = \frac{-g_{0\phi} \pm \sqrt{g_{0\phi}^2 - g_{00}g_{\phi\phi}}}{g_{\phi\phi}}. \quad (3)$$

If $g_{0\phi} < 0$, one root allows a circular orbit in negative time:

$$\Delta T = \frac{-2\pi|g_{\phi\phi}|}{-g_{0\phi} + \sqrt{g_{0\phi}^2 + |g_{\phi\phi}|g_{00}}}. \quad (4)$$

In the following we will apply a similar argument to different scenarios of asymmetrically warped spacetimes.

Warped-Space CTC:

3 Causality of asymmetrically warped spacetimes

We now consider the asymmetrically warped line element with extra dimension “ u ”

$$ds^2 = dt^2 - \sum_i \alpha^2(u) (dx^i)^2 - du^2, \quad (5)$$

$i = 1, 2, 3$, with our brane located at the $u = 0$ submanifold. The warped space-time of (5) allows shortcut geodesics connecting spacelike-separated events on the brane, if $|\alpha(u)| < |\alpha(0)|$ for any $u \neq 0$.

Variants of this warped space-time (5) can be generated by AdS-Schwarzschild or AdS-Reissner-Nordström black holes in the bulk [26, 27], and have been proposed as solutions to the cosmological horizon problem [20], and as a possible way around Weinberg’s no-go theorem for the adjustment of the cosmological constant [27]. They also have been discussed in the context of the gravitational generation of cosmic acceleration [28], and

For the metric (5) there exists a global time function t . Thus, taken by itself the space-time (5) is causally stable and does not allow for CTCs. This can be seen explicitly, when one tries to construct a closed-timelike curve, as we now do.

5D does not Time-Travel

The complete metric in the boosted system is given by the tensor transformation law

$$g'_{\alpha\beta} = \frac{\partial x^\mu}{\partial x'^\alpha} \frac{\partial x^\nu}{\partial x'^\beta} g_{\mu\nu}, \quad (8)$$

where $g_{\mu\nu} = \text{diag}(1, -\alpha^2, -1)$ is the Gauss-normal metric of Eq. (5). Using Eq. (7), the resulting boosted metric is

$$g'_{\mu\nu} = \begin{pmatrix} \gamma^2(1 - \beta^2\alpha^2) & \gamma^2\beta(1 - \alpha^2) & 0 \\ \gamma^2\beta(1 - \alpha^2) & -\gamma^2(\alpha^2 - \beta^2) & 0 \\ 0 & 0 & -1 \end{pmatrix}. \quad (9)$$

Notice that only for $\alpha^2 = 1$ is the metric Lorentz invariant. Such is the case on our brane, but generally not the case on other hypersurfaces, where the limiting velocity as seen by local inhabitants in the rest frame is $\alpha^{-1}(u_j) \equiv \alpha_j^{-1}$. However, these limiting velocities are not invariant under Lorentz boosts defined on our brane.

At first glance the metric (9) seems to belong to the broad class of metrics(1), which includes the Gödel- and Tipler-van-Stockum spacetimes. However, in the case of a boosted asymmetrically warped extra dimension, the variable x is not periodic (unless our universe has the topology of a flat torus). It is thus required to construct an explicit return path to the spacetime point of origin. It is not hard to show that this cannot be done in 5D.

A constructed “geodesic”

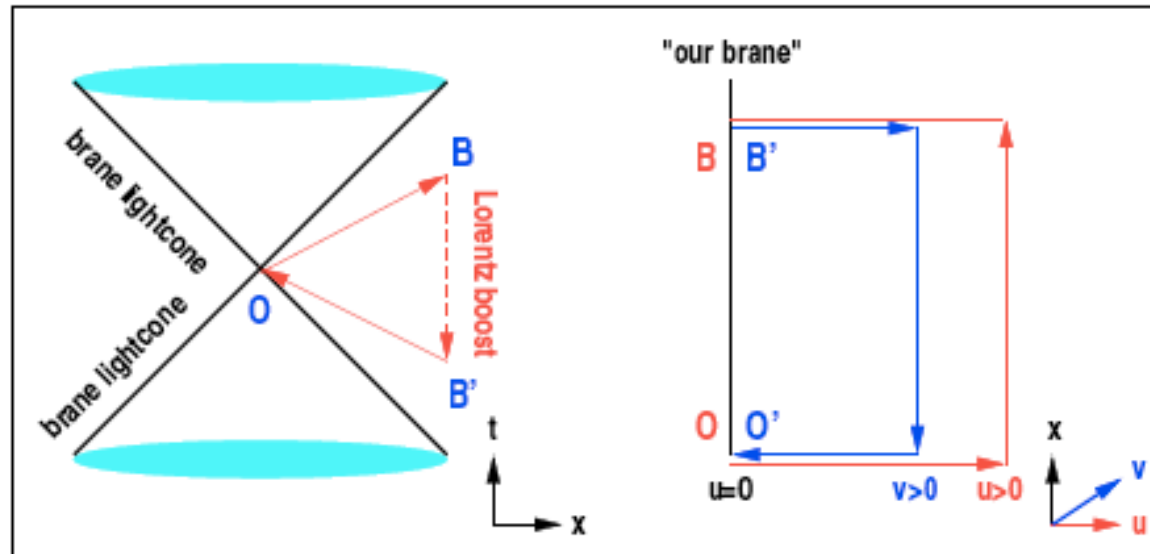


Figure 1: Closed timelike curve in an asymmetrically warped universe: (i) A signal takes a spacelike shortcut via a path of constant $u = u_0$ with $v = 0$ from point O to point B . (ii) A Lorentz boost transforms B into B' with negative time coordinate. (iii) A return shortcut at constant $v = v_0$ with $u = 0$ closes the timelike curve.

It should be stressed that realistic graviton or bulk fermion signals, rather than following restricted bulk trajectories with constant u or v as constructed here, will instead propagate on the path of least action to minimize the travel time. Since the effectively superluminal velocities in our constructed example produced a CTC, we expect that a truly geodesic signal will also generate a CTC.

6D Time Travel

Let “ u ” and “ v ” label the two extra space dimensions. We assume that these dimensions have independent warp factors $\alpha(u)$ and $\eta(v)$, respectively. We further assume that the metric for the u - and v dimensions exhibits the simple form in (5), but in different Lorentz frames. Note that this is natural for any spacetime with two or more extra dimensions, as there is no preferred Lorentz frame from the viewpoint of the brane. In the following we construct this 6-dimensional metric explicitly. We denote by β_{uv} the relative velocity between the two Lorentz frames in which the u and v dimensions assume the simple form (5).

It is easy to show that, given our assumptions, the full 6-dimensional metric has the form

$$ds^2 = \gamma^2 \left\{ (1 - \beta_{uv}^2 \eta^2(v)) dt^2 - 2\beta_{uv} \alpha(u) (\eta^2(v) - 1) dx dt - \alpha^2(u) (\eta^2(v) - \beta_{uv}^2) dx^2 \right\} - du^2 - dv^2.$$

SCIENCE AND TECHNOLOGY NEWS

THE BEST JOBS IN MICROBIOLOGY

NewScientist

May 20-26, 2006



Time travel

At last, an idea we can test



It's a relative concept

The ν_s Time-Traveller:

A natural candidate for a bulk fermion in string theory is an SU(2) singlet “sterile” neutrino. In many particle theories, these sterile neutrinos would mix with the Standard Model neutrinos, and will be generated by neutrino oscillations when neutrinos propagate in space and time. Sterile neutrinos thus provide an accessible probe for the causality properties of extra dimensions. An experiment testing for such properties of spacetime could effectively transform active neutrinos into sterile neutrinos by using the resonant conversion in an increasing matter density known as Mikheev-Smirnov-Wolfenstein (MSW) effect. A neutrino beam of suitably chosen energy could be generated in a beam-dump experiment

Once being converted inside the Earth’s core, the sterile neutrinos will avail shortcuts in extra dimension to minimize the action of the propagation path, and thus effectively propagate a spacelike distance. On their way out of the Earth’s interior the sterile neutrinos are reconverted into active flavors, which could be observed by a neutrino detector :

If the neutrinos have advanced a spacelike distance,

It could be possible to send the signal back to the

point of origin (

before it had been sent off.

Energy Conditions and Consistency

As a check on the consistency of the picture, we should diagnose the stress-energy tensor

$$T_{\mu\nu} = \frac{1}{8\pi G_N} G_{\mu\nu} \quad (16)$$

which sources the extra-dimensional metric, for any pathologies. Thus, our task is to construct the Einstein tensor

$$G_{\mu\nu} = R_{\mu\nu} - \frac{1}{2}g_{\mu\nu}R, \quad (17)$$

There is considerable theoretical prejudice that stable Einstein tensors should satisfy certain “energy conditions”. Defined in terms of

$$\rho = G^{00} \quad \text{and} \quad p_j = G^{jj}, \quad (18)$$

the null, weak, strong and dominant energy conditions state that

$$\text{NEC} : \rho + p^j \geq 0 \quad \forall j; \quad (19)$$

$$\text{WEC} : \rho \geq 0 \quad \text{and} \quad \forall j, \quad \rho + p^j \geq 0; \quad (20)$$

$$\text{SEC} : \forall j, \quad \rho + p^j \geq 0 \quad \text{and} \quad \rho + \sum_j p^j \geq 0; \quad (21)$$

$$\text{DEC} : \rho \geq 0 \quad \text{and} \quad \forall j, \quad p^j \in [\rho, -\rho]. \quad (22)$$

It is not difficult to find a functional form for the warp factors α and η which conserves some of the energy conditions, at least on the brane. One such example is given by $\alpha(u) = 1/(u^2 + c^2)$ and $\eta(v) = 1/(v^4 + c^2)$. For this case the elements of the Einstein tensor on the $v = 0$ slice are shown as a function of u in Fig. 2. The null, weak and dominant energy conditions are conserved on the brane, while the strong energy condition is violated on the brane.

On-brane Off-brane

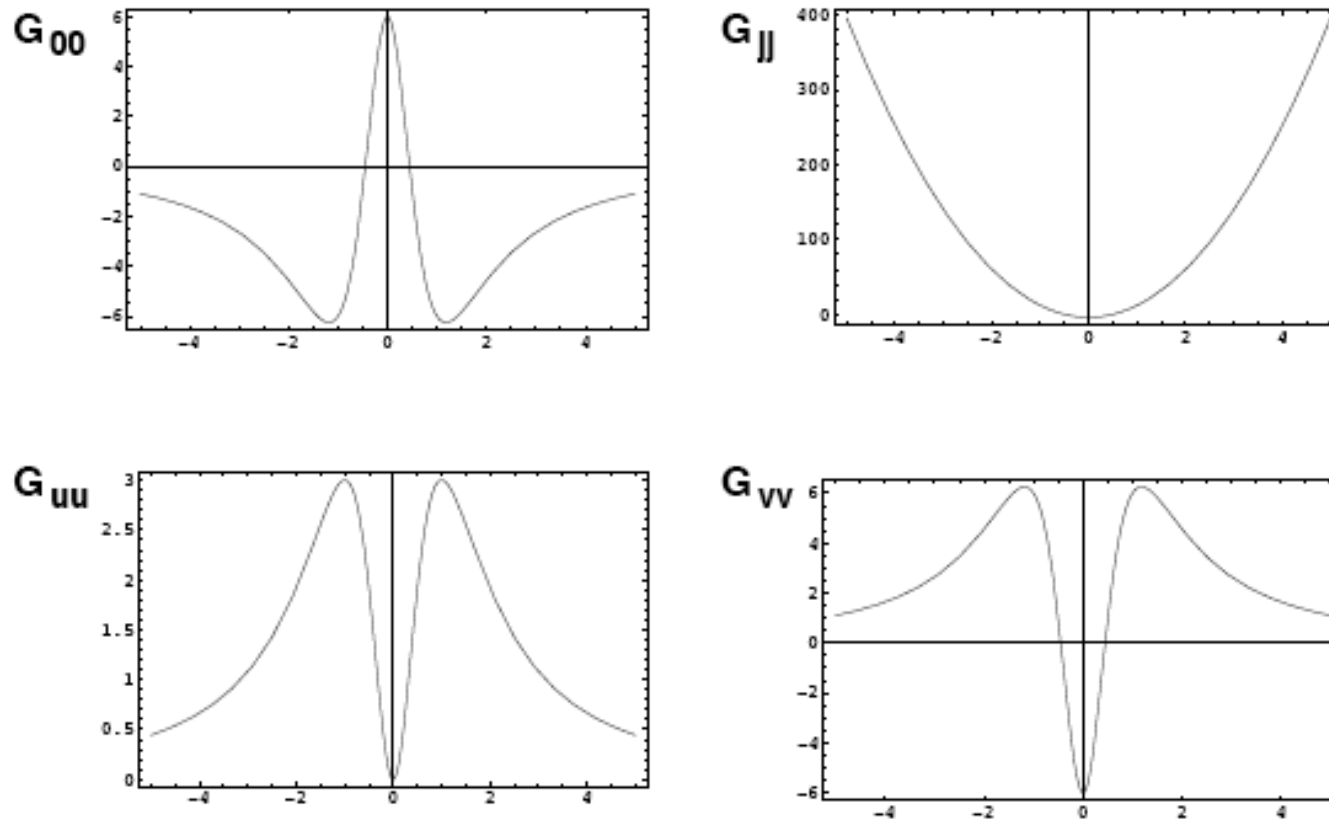


Figure 2: Nonzero elements of the Einstein tensor $G^{\mu\nu}$ on the $v = 0$ slice, as a function of u , for warp factors $\alpha(u) = 1/(u^2 + c^2)$ and $\eta(v) = 1/(v^4 + c^2)$, with $c = 1$. While the null, weak and dominant energy conditions are violated in the bulk, they are conserved on the brane.

In Summary,

Nature has real opportunities

with Sterile Neutrinos

I hope She realizes this!